Phosphorus-31 Chemical Shift Tensors of Phosphinidene Ligands in Ruthenium Carbonyl Cluster Compounds: A ^{31}P Single-Crystal and CP/MAS-NMR Study

Klaus Eichele,[†] Roderick E. Wasylishen,*[,†] John F. Corrigan,[‡] Nicholas J. Taylor,[‡] and Arthur J. Carty[‡]

Contribution from the Department of Chemistry, Dalhousie University, Halifax, Nova Scotia, Canada B3H 4J3, and Guelph-Waterloo Centre for Graduate Work in Chemistry, Department of Chemistry, University of Waterloo, Waterloo, Ontario, Canada N2L 3G1

Received January 31, 1995[⊗]

Abstract: Phosphorus chemical shift tensors of the phosphinidene moiety, formally RP^{2-}, in several solid ruthenium carbonyl clusters have been characterized using slow magic-angle spinning ^{31}P NMR techniques. Typically, the phosphorus nucleus in these systems is highly deshielded relative to the standard reference, 85% H_3PO_4(aq), with isotropic chemical shifts in the range of 200-550 ppm. For one representative cluster, *nido*-$Ru_4(CO)_{13}(\mu_3$-PPh), **2**, ^{31}P NMR studies of a single crystal yielded the principal components of the phosphorus chemical shift (CS) tensor (δ_{11} = 889, δ_{22} = 294, and δ_{33} = 60 ppm) as well as the orientation of the CS tensor. The deshielding is most pronounced when the applied magnetic field, B_0, is oriented approximately parallel to the P-C bond of the PPh moiety, while the greatest shielding occurs when B_0 is approximately perpendicular to the P-C bond and the open face of the *nido*-Ru_4 cluster. The orientation of the phosphorus chemical shift tensor is discussed in the context of Ramsey's theory of nuclear magnetic shielding and the results of extended Hückel molecular orbital calculations. With the P-C bond axis defined as the x-axis, the large deshielding in these clusters is thought to be associated with π_y- and π_z-type orbitals localized on the phosphorus atom of the PPh moiety.

Introduction

Phosphorus-31 NMR spectroscopy is one of the most important techniques available for the characterization of compounds containing phosphorus. In particular, phosphorus chemical shifts (CS) are of primary importance in providing evidence for a specific functional group. There is a wealth of phosphorus CS data from solution NMR studies, and from this data typical chemical shift ranges for a given structural moiety are well-known.[1] Unfortunately, a general understanding of phosphorus chemical shifts is lacking. While modern *ab initio* molecular orbital (MO) calculations of phosphorus chemical shieldings show promise,[2] particularly for small molecules, the potential of these techniques for molecules containing heavy metals is much less certain. Furthermore, the interpretation of the results of theoretical calculations in terms of chemical concepts familiar to chemists is lacking. The last systematic attempt toward obtaining a general understanding of phosphorus chemical shifts was presented by Letcher and Van Wazer,[1a,3] almost 30 years ago! Clearly, a new effort is long overdue.

In order to improve our understanding of phosphorus chemical shifts, it is our basic premise that one should attempt to characterize the shielding tensor as opposed to its average value or trace. In general, the three principal components of the CS tensor and its precise orientation are more sensitive to subtle structural changes and potentially provide detailed insight into the electronic structure about the nucleus. Indeed, the ultimate test for any theoretical description of phosphorus chemical shifts will involve the complete tensor rather than solely its trace.

Modern solid-state NMR techniques provide experimentalists with an opportunity to measure the three principal components of CS tensors.[4] Information concerning the orientation of a chemical shift tensor is sometimes available from symmetry arguments or dipolar-chemical shift NMR; however, the most definitive information is obtained from NMR studies of single crystals. Surprisingly, there are only two examples of single-

* Address correspondence to this author. Phone: 902-494-2564. Fax: 902-494-1310. E-mail: RODW@AC. DAL. CA.

[†] Dalhousie University.

[‡] University of Waterloo.

[⊗] Abstract published in *Advance ACS Abstracts*, June 1, 1995.

(1) (a) Van Wazer, J. R.; Letcher, J. H. In *Topics in Phosphorus Chemistry*; Grayson, M., Griffith, E. J., Eds.; Interscience: New York, 1967; Vol. 5, pp 169-226. (b) Pregosin, P. S.; Kunz, R. W. In *NMR Basic Principles and Progress*; Diehl, P., Fluck, E., Kosfeld, R., Eds.; Springer-Verlag: Berlin, 1979; Vol. 16. (c) Gorenstein, D. G. In *Progress in NMR Spectroscopy*; Emsley, J. W., Feeney, J., Sutcliffe, L. H., Eds.; Pergamon Press: Oxford, U.K., 1983; Vol. 16, pp 1-98. (d) *Phosphorus-31 NMR, Principles and Applications*; Gorenstein, D., Ed.; Academic Press: Orlando, FL, 1984. (e) *Phosphorus-31 NMR Spectroscopy in Stereochemical Analysis, Organic Compounds and Metal Complexes*; Verkade, J. G., Quin, L. D., Eds.; Methods in Stereochemical Analysis 8; VCH Publishers, Inc.: Deerfield Beach, FL, 1987. (f) Dixon, K. R. In *Multinuclear NMR*; Mason, J., Ed.; Plenum Press: New York, 1987; pp 369-402. (g) *Phosphorus-31 NMR Spectral Properties in Compound Characterization and Structural Analysis*; Verkade, J. G., Quin, L. D., Eds.; VCH Publishers, Inc.: Deerfield Beach, FL, 1994.

(2) (a) Chesnut, D. B. *Phosphorus-31 NMR Spectroscopy in Stereochemical Analysis, Organic Compounds and Metal Complexes*; Verkade, J. G., Quin, L. D., Eds.; Methods in Stereochemical Analysis 8; VCH Publishers, Inc.: Deerfield Beach, FL, 1987; pp 185-204. (b) Jameson, C. J.; Mason, J. In *Multinuclear NMR;* Mason, J., Ed.; Plenum Press: New York, 1987; pp 51-88. (c) Kutzelnigg, W.; Fleischer, U.; Schindler, M. In *NMR Basic Principles and Progress*; Diehl, P., Fluck, E., Günther, H., Kosfeld, R., Seelig, J., Eds.; Springer-Verlag: Heidelberg, 1990; Vol. 23, pp 165-262. (d) Chesnut, D. B. *Annu. Rep. NMR Spectrosc.* **1989**, *21*, 51-97. (e) *Nuclear Magnetic Shieldings and Molecular Structure*; Tossell, J. A., Ed.; NATO ASI Series C; Kluwer Academic Publishers: Dordrecht, 1993; Vol. 386.

(3) Letcher, J. H.; Van Wazer, J. R. *J. Chem. Phys.* **1966**, *44*, 815-29; **1966**, *45*, 2916-25; **1966**, *45*, 2926-29.

(4) (a) Carty, A. J.; Fyfe, C. A.; Lettinga, M.; Johnson, S.; Randall, L. H. *Inorg. Chem.* **1989**, *28*, 4120-24. (b) Power, W. P.; Wasylishen, R. E. *Inorg. Chem.* **1992**, *31*, 2176-83. (c) Lindner, E.; Fawzi, R.; Mayer, H. A.; Eichele, K.; Hiller, W. *Organometallics* **1992**, *11*, 1033-43. (d) Eckert, H.; Liang, C. S.; Stucky, G. D. *J. Phys. Chem.* **1989**, *93*, 452-7. (e) Grimmer, A. R. *J. Chim. Phys.* **1992**, *89*, 413-21.

0002-7863/95/1517-6961$09.00/0

crystal ^{31}P NMR studies on transition metal complexes of phosphorus ligands, specifically, Wilkinson's catalyst, $Rh(PPh_3)_3Cl$,[5] and dinitrato tricyclohexylphosphine mercury(II), $Hg(PCy_3)(NO_3)_2$.[6]

The objective of the present study is to experimentally characterize the phosphorus chemical shifts of the phosphinidene ligand, formally RP^{2-}. The isotropic ^{31}P chemical shifts of phosphinidenes generally indicate significant deshielding but vary over an extremely wide range, from 66 to 1362 ppm.[7] To fully appreciate this range of chemical shifts, it might be useful to consider that the chemical shift of the free phosphorus atom, the species of highest ^{31}P shielding, is −632 ppm, while the chemical shift of the *bare* ^{31}P nucleus, P^{15+}, is 328 ppm.[8] Although the phosphorus nucleus of phosphinidene units is the least shielded phosphorus species known, no thorough interpretation of these remarkable effects has been presented.

We have carried out solid-state ^{31}P NMR studies of powder samples of ruthenium cluster compounds containing the phosphinidene unit to obtain the principal components of the chemical shift tensor. In addition, we carried out a single-crystal ^{31}P NMR study of a representative Ru cluster containing the RP^{2-} unit to obtain the orientation of the phosphorus chemical shift tensor in the molecular frame. Expressions first derived by Ramsey[9] and a simple analysis of a qualitative frontier orbital MO scheme of the RP^{2-} unit are used to provide a first step toward understanding the factors determining the phosphorus chemical shifts of phosphinidene groups.

Experimental Section

Sample Preparation. The preparations of $Ru_8(CO)_{21}(\mu_6\text{-P})(\mu_4\text{-PPh})(\mu_2\text{-PPh}_2)$, **1**,[10] *nido*-$Ru_4(CO)_{13}(\mu_3\text{-PPh})$, **2**,[11] *nido*-$Ru_4(CO)_{13}[\mu_3\text{-PN}(i\text{Pr})_2]$, **3**,[12] *nido*-$Ru_4(CO)_{10}(\mu\text{-CO})_2\{\mu_3\text{-}\eta^1,\eta^1,\eta^2\text{-P(Ph)C(C}{\equiv}\text{CMe)CMe}\}$, **4**,[13] *closo*-$Ru_4(CO)_9(\mu\text{-CO})_2(\mu_4\text{-PPh})(\mu_4\text{-}\eta^1,\eta^2,\eta^1,\eta^2\text{-Ph-C}{\equiv}\text{C-Ph})$, **5**,[14] *closo*-$Ru_4(CO)_{10}(\mu_4\text{-PPh})(\mu_4\text{-}\eta^1,\eta^1,\eta^3,\eta^3\text{-Me}_3\text{Si-C}{\equiv}\text{C-C}{\equiv}\text{C-SiMe}_3)$, **6**,[13] and *closo*-$Ru_4(CO)_{10}(\mu\text{-CO})(\mu_4\text{-PPh})(\mu_4\text{-}\eta^1,\eta^1,\eta^1,\eta^1\text{-Ph-N}{=}\text{N-Ph})$, **7**,[15] have been described in the literature previously. Dark red crystals of **2** were grown from the slow evaporation of $CDCl_3$ solutions at 294 K. Compound **2** crystallizes in the orthorhombic, noncentrosymmetric space group $P2_12_12_1$, with $a = 11.031$ Å, $b = 12.366$ Å, and $c = 18.094$ Å, $Z = 4$.[11] A crystal measuring approximately 2 × 2 × 3 mm was used for the single-crystal NMR experiments. The orientation of the crystal axis system was determined using an X-ray diffractometer to index the crystal faces. The single crystal was then glued onto a hollow three-sided alumina cube measuring 4 mm on each side. The crystal was mounted on its $0\bar{1}0$ face to the *XY* plane of the crystal holder and on the small $00\bar{1}$ face to the *XZ* plane of the hollow cube, such that the *a*, *b*, and *c* crystal axes were approximately parallel to the -*X*, *Z*, and *Y* axes of the hollow cube, respectively (Figure 1).

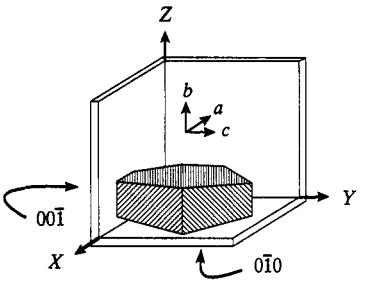

Figure 1. Illustration of the relative orientations of the orthorhombic crystal axis system (*a*, *b*, and *c*) and the crystal holder, referred to as the orthogonal NMR cube frame (*X*, *Y*, and *Z*).

NMR Experiments. Solid-state ^{31}P NMR experiments were carried out at 81.03 MHz using a Bruker MSL-200 spectrometer ($B_0 = 4.7$ T). The single-crystal ^{31}P NMR spectra were obtained using an automated single-crystal goniometer probe from Doty Scientific. The cube mount was placed into a hollow cubic receptacle in the goniometer of the probe, with the rotation axis perpendicular to the magnetic field. Rotations about the three orthogonal cube axes *X*, *Y*, and *Z* were performed in 9° intervals, controlled by an external stepper motor placed underneath the probe. The ^{31}P NMR spectra were acquired after cross-polarization (CP) using the Hartmann−Hahn match condition and under high-power proton decoupling, using ^1H pulse widths of 3.2 μs, contact times of 5 ms and a flip-back pulse on the ^1H channel.[16] Recycle delays of at least 40 min were used since the rate of ^1H spin−lattice relaxation was found to be very slow. The CP efficiency was found to be strongly dependent on the crystal orientation in B_0 (*vide infra*), and for several orientations single-pulse excitation with high-power ^1H decoupling was employed. Typically, at least eight FIDs were acquired, using a sweep width of 83 kHz and a time domain size of 2 K. Approximately six weeks of spectrometer time was required to acquire the single-crystal NMR data! The ^{31}P NMR line widths were on average 1.0 ± 0.4 kHz. Details concerning the analysis of single-crystal NMR experiments performed in our laboratory can be found in the literature.[6,17]

Phosphorus-31 CP/magic-angle spinning (MAS) NMR spectra were acquired using a Bruker double-bearing MAS probe, with 3 μs proton pulse widths and contact times of 3−5 ms. Chemical shifts were referenced with respect to external 85% aqueous H_3PO_4 by setting the peak of external $NH_4H_2PO_4$ to 0.8 ppm. The analysis of the spinning-sideband intensities in the MAS−NMR spectra was carried out using a SIMPLEX least-squares routine based on the Herzfeld−Berger method,[18] with extended ϱ, μ tables for spinning sidebands up to ±15th order and $\mu \leq 30$.[19] Calculations of the MAS spectra were performed following the direct time-domain calculation method outlined by Mehring[20] and Clayden.[21] For this purpose, a program was written in C. The calculations were performed on a 80486 microprocessor, requiring approximately 90 s.

Molecular Orbital Calculations. Extended Hückel molecular orbital (EHMO) calculations were performed using the CACAO program with standard parameters.[22] The involvement of *d* orbitals on phosphorus was not considered. Bond lengths and angles were obtained from the X-ray structure analysis of **2**,[11] but with idealized C_s symmetry. The P−H bond length was fixed at 1.40 Å.

(5) Naito, A.; Sastry, D. L.; McDowell, C. A. *Chem. Phys. Lett.* **1985**, *115*, 19−23.
(6) Lumsden, M. D.; Eichele, K.; Wasylishen, R. E.; Cameron, T. S.; Britten, J. F. *J. Am. Chem. Soc.* **1994**, *116*, 11129−36.
(7) Carty, A. J.; MacLaughlin, S. A.; Nucciarone, D. *Phosphorus-31 NMR Spectroscopy in Stereochemical Analysis, Organic Compounds and Metal Complexes*; Verkade, J. G., Quin, L. D., Eds.; Methods in Stereochemical Analysis 8; VCH Publishers, Inc.: Deerfield Beach, FL, 1987; pp 559−619.
(8) Jameson, C. J.; De Dios, A.; Jameson, A. K. *Chem. Phys. Lett.* **1990**, *167*, 575−82.
(9) Ramsey, N. F. *Phys. Rev.* **1950**, *78*, 699−703; **1952**, *86*, 243−6.
(10) Van Gastel, F.; Taylor, N. J.; Carty, A. J. *Inorg. Chem.* **1989**, *28*, 384−8.
(11) Cherkas, A. A.; Corrigan, J. F.; Doherty, S.; MacLaughlin, S. A.; van Gastel, F.; Taylor, N. J.; Carty, A. J. *Inorg. Chem.* **1993**, *32*, 1662−70.
(12) Corrigan, J. F.; Doherty, S.; Taylor, N. J.; Carty, A. J. *J. Am. Chem. Soc.* **1994**, *116*, 9799−800.
(13) Corrigan, J. F.; Doherty, S.; Taylor, N. J.; Carty, A. J. *Organometallics* **1993**, *12*, 1365−77.
(14) Lunniss, J.; MacLaughlin, S. A.; Taylor, N. J.; Carty, A. J.; Sappa, E. *Organometallics* **1985**, *4*, 2066−8.
(15) Corrigan, J. F.; Doherty, S.; Taylor, N. J.; Carty, A. J. *J. Chem. Soc., Chem. Commun.* **1991**, 1640−1.
(16) Tegenfeldt, J.; Haeberlen, U. *J. Magn. Reson.* **1979**, *36*, 453−7.
(17) (a) Power, W. P.; Mooibroek, S.; Wasylishen, R. E.; Cameron, T. S. *J. Phys. Chem.* **1994**, *98*, 1552−60. (b) Eichele, K.; Wasylishen, R. E. *J. Phys. Chem.* **1994**, *98*, 3108−13. (c) Eichele, K.; Wu, G.; Wasylishen, R. E.; Britten, J. F. *J. Phys. Chem.* **1995**, *99*, 1030−7.
(18) Herzfeld, J.; Berger, A. E. *J. Chem. Phys.* **1980**, *73*, 6021−30.
(19) (a) Kentgens, A. University of Nijmegen, The Netherlands. (b) Power, W. P.; Wasylishen, R. E. unpublished results.
(20) Mehring, M. *Principles of High Resolution NMR in Solids*, 2nd ed.; Springer Verlag: Berlin, 1983.
(21) Clayden, N. J.; Dobson, C. M.; Lian, L.-Y.; Smith, D. J. *J. Magn. Reson.* **1986**, *69*, 476−87.
(22) Mealli, C.; Proserpio, D. M. *J. Chem. Educ.* **1990**, *67*, 399−402.

Chart 1

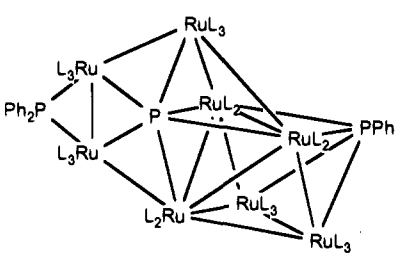

1

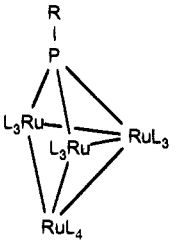

2 R = Ph

3 R = N(*i*Pr)$_2$

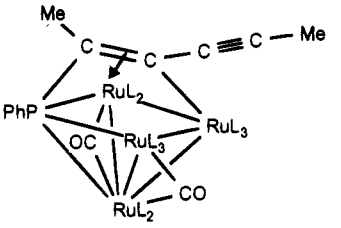

4

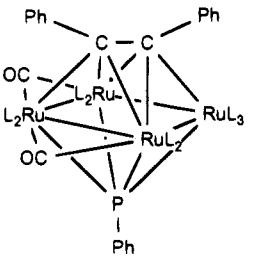

5

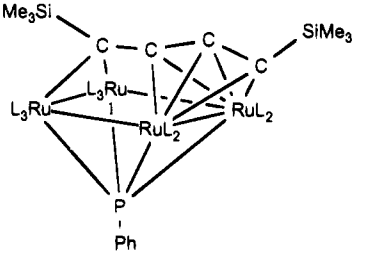

6

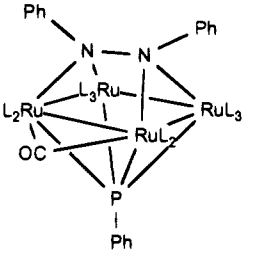

7

L = CO

Table 1. Principal Components of the Phosphorus Chemical Shift Tensors (in ppm) for the Phosphinidene-Containing Cluster Compounds **1**–**7** as Determined by CP/MAS and Single-Crystal ^{31}P NMR Spectroscopy[a]

compound		δ_{iso}	δ_{11}	δ_{22}	δ_{33}	Ω^b
$Ru_8(CO)_{21}(\mu_6\text{-P})(\mu_4\text{-PPh})(\mu_2\text{-PPh}_2)$	**1**	214 (μ_2)	562	139	−58	620
		539 (μ_4)	1122	317	178	944
		565 (μ_6)	995	512	188	807
nido-$Ru_4(CO)_{13}(\mu_3\text{-PPh})$	**2**	414[c]	889	294	60	829
		414[d]	890	298	53	837
nido-$Ru_4(CO)_{13}[\mu_3\text{-PN}(i\text{Pr})_2]$	**3**	442	880	294	151	729
nido-$Ru_4(CO)_{10}(\mu\text{-CO})_2\{\mu_3\text{-}\eta^1,\eta^1,\eta^2\text{-P(Ph)C(C≡CMe)CMe}\}$	**4**	48	185	9	−51	236
closo-$Ru_4(CO)_9(\mu\text{-CO})_2(\mu_4\text{-PPh})(\mu_4\text{-}\eta^1,\eta^2,\eta^1,\eta^2\text{-Ph-C≡C-Ph})$	**5**	235	631	66	8	623
closo-$Ru_4(CO)_{10}(\mu_4\text{-PPh})(\mu_4\text{-}\eta^1,\eta^1,\eta^3,\eta^3\text{-Me}_3\text{Si-C≡C-C≡C-SiMe3})$	**6**	457	1011	232	126	885
closo-$Ru_4(CO)_{10}(\mu\text{-CO})(\mu_4\text{-PPh})(\mu_4\text{-}\eta^1,\eta^1,\eta^1,\eta^1\text{-Ph-N=N-Ph})$	**7**	353	840	210	7	837

[a] Chemical shifts are given with respect to 85% aqueous phosphoric acid and conform to the high-frequency positive convention. Errors in the principal components are estimated to be 10 ppm for the values obtained from the MAS spectra, and 2 ppm for the values obtained from the single-crystal experiment. [b] Span of the chemical shift tensor, $\Omega = \delta_{11} - \delta_{33}$. [c] Data obtained from single-crystal ^{31}P NMR experiment. [d] Data obtained from ^{31}P CP/MAS–NMR spectra.

Phosphorus-31 chemical shielding tensors of HP^{2-} have been calculated using an efficient implementation[23] of the GIAO method[24] incorporated in the TEXAS 90 *ab initio* program package.[25] A 6-311G basis set was used, augmented with two sets of polarization functions on both atoms. The P–H bond distance was optimized at this level of theory, resulting in an equilibrium distance of 1.463(1) Å. Absolute chemical shieldings have been converted to chemical shifts using the absolute chemical shielding of 85% aqueous H_3PO_4, $\sigma = 328.35$ ppm.[8] All shielding calculations were performed using an IBM RS6000/580 workstation.

Results and Discussion

Solid-State ^{31}P NMR of Powder Samples. The principal components of the phosphorus chemical shift tensors obtained from CP/MAS–NMR studies of powder samples of compounds **1**–**7** (Chart 1) as well as a single-crystal NMR study of compound **2** are summarized in Table 1. For most of these cluster compounds, phosphorus is present as a μ_3- or μ_4-bridging phosphinidene group. With the exception of compound **4**, the phosphorus chemical shift tensors of each compound exhibit considerable anisotropy, *i.e.*, a large dependence of the chemical shift on the orientation of the molecule in B_0, as measured by the span Ω of the CS tensor.

Compound 1. Cluster compound **1** serves as an excellent example to demonstrate the dramatic differences in the phosphorus chemical shift tensors of different types of phosphorus ligands. The three types of phosphorus ligands in **1** are formally derived from triphenylphosphine by the successive loss of a phenyl group.[10] As the ^{31}P CP/MAS–NMR spectrum of compound **1** demonstrates (Figure 2), the successive loss of phenyl groups results in deshielding at phosphorus, accompanied by an increase in the chemical shift anisotropy. Compared to other PR_2 ligands bridging Ru–Ru bonds,[4a,26] the phosphorus of the μ_2-bridging phosphido ligand in **1** is deshielded and exhibits a relatively large chemical shift anisotropy. More

(23) Wolinski, K.; Hinton, J. F.; Pulay, P. *J. Am. Chem. Soc.* **1990**, *112*, 8251–60.
(24) Ditchfield, R. *Mol. Phys.* **1974**, *27*, 789–807.
(25) Pulay, P. *Theor. Chim. Acta* **1979**, *50*, 299–312.
(26) Carty, A. J. *Adv. Chem. Ser.* **1982**, *196*, 163–93.

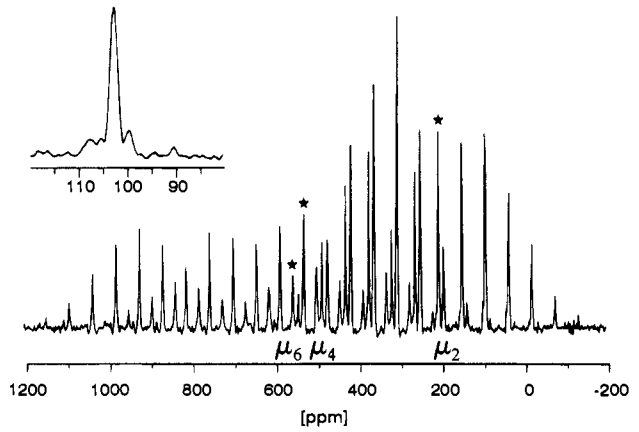

Figure 2. ^{31}P CP/MAS−NMR spectrum of $Ru_8(CO)_{21}(\mu_6\text{-P})(\mu_4\text{-PPh})(\mu\text{-PPh}_2)$, **1**, obtained at 4.7 T with a MAS rate of 4.5 kHz, 1500 scans, 200 kHz sweep width, and 20 s recycle delay. The isotropic ^{31}P chemical shifts of the μ_6-, μ_4-, and μ_2-bridging phosphorus species are indicated by asterisks. The insert shows an expansion of the second order low-frequency spinning sideband due to the μ_2-P, illustrating the presence of ^{99,101}Ru satellites.

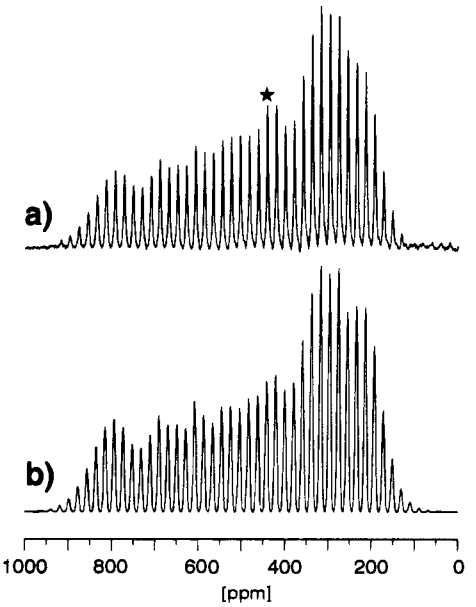

Figure 3. ^{31}P CP/MAS−NMR spectrum of *nido*-$Ru_4(CO)_{13}[\mu_3\text{-PN}(i\text{Pr})_2]$, **3**, obtained at 4.7 T with a MAS rate of 1.68 kHz: (a) experimental spectrum, 934 scans, 125 kHz sweep width, and 8 s recycle delay and (b) spectrum calculated using the values given in Table 1. The isotropic peak is marked by an asterisk.

detailed solid-state ^{31}P NMR investigations of powder and single-crystal samples containing phosphido groups will be described in a later paper.

The μ_4-PPh group of **1** exhibits a very large chemical shift anisotropy; together with the data in Table 1 obtained for the other phosphinidene complexes, these chemical shift anisotropies are only surpassed by bis(tri-2,4,6-*tert*-butylphenyl)diphosphene, R-P=P-R.[27,28] The phosphorus nucleus of the μ_6-P atom is less shielded than that of the μ_4-PPh group but less anisotropic. While most of the ^{31}P chemical shifts reported for genuine metal phosphides with infinite solid state structures indicate fairly shielded phosphorus nuclei, $\delta_{iso} = -6$ to -262 ppm,[29] the phosphide in compound **1** and similar phosphides[30] exhibit strong deshielding. At present, there is no interpretation of the factors influencing ^{31}P chemical shifts of phosphides.

The peak in the ^{31}P CP/MAS−NMR spectrum of **1** assigned to the μ_4-PPh ligand is split into a doublet, ascribed to indirect ^{31}P,^{31}P spin−spin coupling with the μ_6-P ligand, $J(\mu_6\text{-}^{31}\text{P}, \mu_4\text{-}^{31}\text{P}) = 150$ Hz. There is no evidence of $J(^{31}\text{P},^{31}\text{P})$ from the peak assigned to the μ_2-PPh_2 group. The peak due to μ_6-P is severely broadened by $J(\mu_6\text{-P}, \mu_4\text{-P})$. In addition, the peaks associated with the μ_6-P ligand are complicated by ^{99,101}Ru,^{31}P spin−spin coupling. Several different spin groupings of the PRu_6 fragment are possible, since the natural abundance of ^{99}Ru (I = 5/2) and ^{101}Ru (I = 5/2) is 12.7% and 17.1%, respectively. Thus it is not surprising that only a broad ^{31}P NMR peak was observed for the μ_6-P moiety. In contrast, the ^{31}P NMR peak due to the μ_2-PPh_2 unit exhibits splitting due to coupling to ^{99}Ru and ^{101}Ru (Figure 2, insert).[31] Although both Ru atoms are crystallographically nonequivalent, they are structurally similar and an average $J(^{99,101}\text{Ru},^{31}\text{P})$ of 170 Hz may be deduced from the spectrum. This coupling constant is relatively large, as compared to the few other J(Ru,P) coupling constants reported to date.[31] In solution ^{31}P NMR studies, indirect couplings involving ^{99}Ru or ^{101}Ru are not observed because of extremely efficient quadrupolar relaxation modulated by molecular tumbling.

Compounds 2 and 3. The CS anisotropy for the phosphorus of the *nido*-clusters **2** and **3** is also large (Table 1). Since the molecular structure does not contain a higher-order rotation axis (*e.g.*, C_3),[11] the CS tensors are also clearly not axially symmetric. For compound **2**, a single-crystal ^{31}P NMR study was carried out (*vide infra*). The principal components of the phosphorus CS tensor obtained from the MAS spectrum of **2** and the single-crystal experiment are in excellent agreement (Table 1). The phosphorus nucleus in an amino-substituted analogue of **2**, *nido*-$Ru_4(CO)_{13}[\mu_3\text{-PN}(i\text{Pr})_2]$, **3**, is deshielded by 30 ppm compared to **2**. Analysis of the ^{31}P CP/MAS spectrum shown in Figure 3 indicates that this deshielding is associated with δ_{33}. Although one might expect to observe indications of the ^{31}P,^{14}N dipolar interaction in the MAS and static ^{31}P NMR spectra,[32] we could not detect such effects. Observation of ^{31}P,^{14}N dipolar splittings in the ^{31}P NMR spectrum of a static powder sample can provide valuable information regarding the relative orientations of the ^{31}P,^{14}N internuclear vector and the ^{31}P chemical shift tensor.[33]

Compounds 4−7. These compounds contain μ_4-bridging phosphinidene groups. They were prepared from the *nido*-cluster **2** by the addition of diynes or hetero-olefins to the Ru_3P open face, followed by skeletal rearrangements. With the exception of compound **4**, all exhibit large ^{31}P chemical shift anisotropies (Table 1). For compound **4**, the phosphorus isotropic chemical shift and the CS anisotropy indicate dramatic changes in structure as one goes from **2** to **4**. Indeed, the phosphorus in **4** is better described as a phosphido ligand than a phosphinidene unit (see Chart 1). It is similar to other phosphido groups, where the substituents at phosphorus undergo

(27) Zilm, K. W.; Webb, G. G.; Cowley, A. H.; Pakulski, M.; Orendt, A. *J. Am. Chem. Soc.* **1988**, *110*, 2032−8.

(28) (a) Challoner, R.; Nakai, T.; McDowell, C. A. *J. Magn. Reson.* **1991**, *94*, 433−8. (b) Nakai, T.; Challoner, R.; McDowell, C. A. *Chem. Phys. Lett.* **1991**, *180*, 13−8. (c) Challoner, R.; Nakai, T.; McDowell, C. A. *J. Chem. Phys.* **1991**, *94*, 7038−45.

(29) Duncan, T. M. *A Compilation of Chemical Shift Anisotropies*; The Farragut Press: Chicago, 1990.

(30) Ho, J.; Rousseau, R.; Stephan, D. W. *Organometallics* **1994**, *13*, 1918−26.

(31) Eichele, K.; Wasylishen, R. E.; Corrigan, J. F.; Doherty, S.; Sun, Y.; Carty, A. J. *Inorg. Chem.* **1993**, *32*, 121−3.

(32) (a) Power, W. P.; Wasylishen, R. E.; Curtis, R. D. *Can. J. Chem.* **1989**, *67*, 454−9. (b) Power, W. P.; Lumsden, M. D.; Wasylishen, R. E. *Inorg. Chem.* **1991**, *30*, 2997−3002.

(33) (a) Eichele, K.; Lumsden, M. D.; Wasylishen, R. E. *J. Phys. Chem.* **1993**, *97*, 8909−16. (b) Eichele, K.; Wasylishen, R. E. *J. Magn. Reson. A* **1994**, *106*, 46−56.

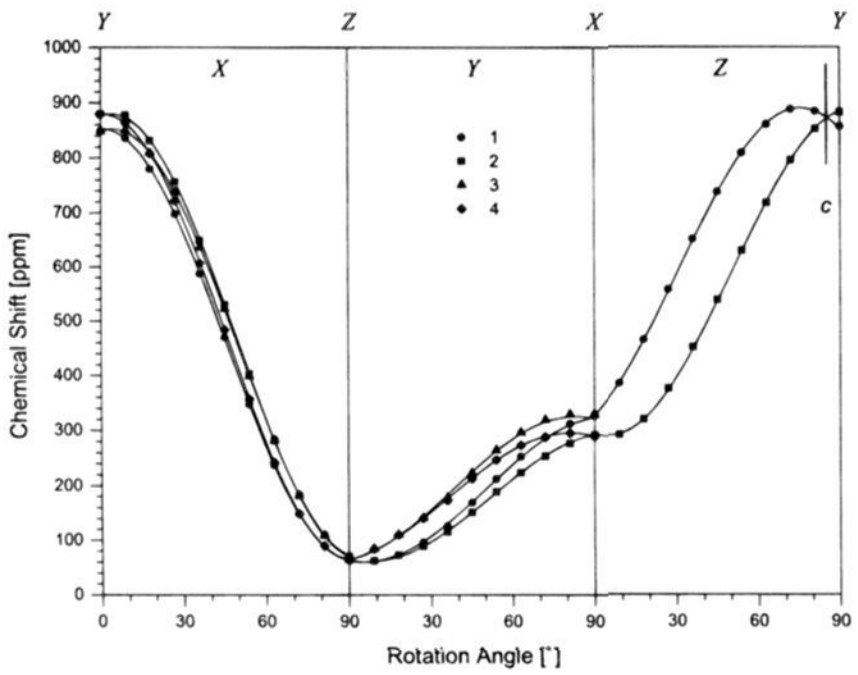

Figure 4. Change of the ^{31}P chemical shift as the single crystal of *nido*-$Ru_4(CO)_{13}(\mu_3$-PPh), **2**, is rotated sequentially about the NMR cube axes *X*, *Y*, and *Z* perpendicular to the external magnetic field. The rotation about *X* starts with *Y* being along the field and ends with *Z* being parallel to B_0, as indicated on the top. The labels 1−4 correspond to the magnetically nonequivalent crystallographic sites (*cf.* Figure 5).

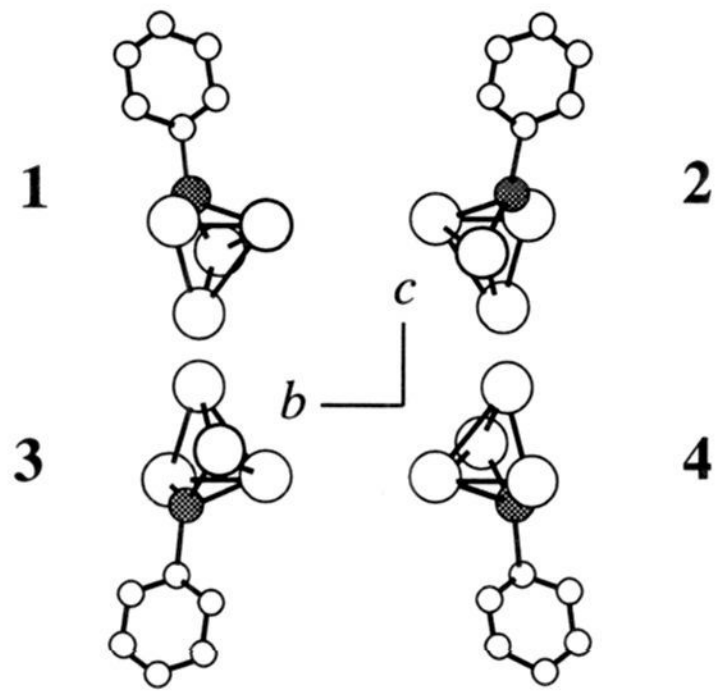

Figure 5. Projection of the four crystallographically equivalent but magnetically nonequivalent molecules of the unit cell of *nido*-$Ru_4(CO)_{13}(\mu_3$-PPh), **2**, into the *bc* plane. The *a* axis points away from the viewer. Note that the individual molecules have been moved closer to each other to facilitate enlargement.

additional bonding interactions with the cluster fragment. Such interactions appear to result in shielding.[11,34]

Cluster **5** has an electron count of 62 cluster valence electrons (CVE), which is two short of that required by the 18-electron rule. Such electron-deficient, "unsaturated" clusters exhibit ^{31}P NMR chemical shifts at lower frequencies compared to those of normal 64 CVE clusters containing μ_4-PPh groups.[13,35] This feature has been ascribed to unusual electronic effects analogous to ring currents in aromatic systems (*vide infra*).

The μ_4-bridging phosphinidene groups of **6** and **7** exhibit phosphorus chemical shifts which are considered as being typical for μ_4-PR ligands bridging an electron-precise Ru_4 square-planar face.[13] As in the case of the μ_3-bridging PR ligands in **2**, **3**, and the μ_4-PR group in **1**, the phosphorus CS tensors are characterized by values of δ_{11} in the range of 800−1100 ppm and CS tensors that are clearly not axially symmetric. Also, the ^{31}P CS tensors of the μ_4-bridging phosphorus species are similar to those of the μ_3-bridging ligands and hence do not indicate any fundamental difference between these bridging modes.

Single-Crystal ^{31}P NMR of 2. In order to obtain information about the orientation of the phosphorus CS tensor of a typical phosphinidene group we have carried out a single-crystal ^{31}P NMR study of compound **2**. The variations in the ^{31}P chemical shift as the crystal was rotated sequentially about an axis perpendicular to the external magnetic field are portrayed in Figure 4. Compound **2** crystallizes with four crystallographically equivalent molecules per unit cell.[11] The relative orientations of the four molecules in the unit cell are shown in Figure 5. For all four molecules, the P−C bond lies approximately along the *c* axis, while the normal to the open face of the *nido*-cluster is oriented toward the *b* direction. Since the three orthogonal 2_1 screw axes of the space group parallel to the crystal axes are nonintersecting, no further symmetry elements are generated, and the four molecules are magnetically nonequivalent. Hence, for a general orientation of the crystal with respect to the magnetic field, four peaks were observed. For rotations about a crystal axis corresponding to one of the screw axes, the molecules are pairwise magnetically equivalent and only two peaks were observed. When the external magnetic field is parallel to one of the crystal axes, all molecules are equivalent and only one peak is detected (*cf.* the intersection of the lines at *Z*(85°) in Figure 4c).

The rotation pattern shown in Figure 4 reveals considerable information about the phosphorus CS tensor prior to a detailed analysis. For the rotation about the crystal holder's *X* axis, B_0 starts parallel to the crystal holder's *Y* axis, which in turn is close to the crystal *c* axis (*cf.* Figure 1). The ^{31}P NMR chemical shifts measured for this orientation are similar to the values obtained for the direction of least shielding, δ_{11}, as determined from the ^{31}P CP/MAS−NMR spectrum. This indicates that δ_{11} is approximately along the P−C bond. Furthermore, at *X*(90°), B_0 is parallel to the crystal holder's $-Z$ axis, corresponding to the crystal *-b* axis. At this orientation, ^{31}P chemical shift values close to δ_{33} were observed, hence the direction of highest shielding is roughly perpendicular to the open face of the *nido*-cluster.

Once the magnetically distinct ^{31}P sites were assigned and traced through all three rotations,[36] the chemical shift data were linear least-squares fitted to eq 1

$$\delta(\phi_i) = A_i + B_i \cos 2\phi_i + C_i \sin 2\phi_i \qquad (1)$$

where ϕ_i is the rotation angle and $i = X$, Y, or Z is the cube axis about which the rotation occurs. The least-squares coefficients A_i,B_i,C_i are given in Table 2. They were used to construct the corresponding phosphorus CS tensors in the cube axis system[37]

$$\delta_{ii} = \frac{1}{2}(A_j - B_j + A_k + B_k)$$

$$\delta_{ij} = -C_k \qquad (2)$$

(34) (a) Corrigan, J. F.; Dinardo, M.; Doherty, S.; Carty, A. J. *J. Cluster Sci.* **1992**, *3*, 313−32. (b) Corrigan, J. F.; Taylor, N. J.; Carty, A. J. *Organometallics* **1994**, *13*, 3778−81.

(35) (a) Jaeger, T.; Aime, S.; Vahrenkamp, H. *Organometallics* **1986**, *5*, 245−52. (b) Field, J. S.; Haines, R. J.; Smit, D. N. *J. Chem. Soc., Dalton Trans.* **1988**, 1315−30.

(36) Carter, C. M.; Facelli, J. C.; Alderman, D. W.; Grant, D. M.; Dalley, N. K.; Wilson, B. E. *J. Chem. Soc., Faraday Trans. 1* **1988**, *84*, 3673−90.

(37) Kennedy, M. A.; Ellis, P. D. *Concepts Magn. Reson.* **1989**, *1*, 35−47, 109−29.

Table 2. Least-Squares Parameters (in ppm) Obtained from the Curve Fitting of the Rotation Patterns shown in Figure 4 to eq 1[b]

rotation axis	curve	A	B	C
X[a]	(1)	459.8 (0.8)	392.6 (1.0)	−18.5 (1.1)
	(2)	473.2 (1.0)	405.8 (1.4)	29.9 (1.5)
	(3)	460.1 (1.3)	391.2 (1.8)	34.8 (1.9)
	(4)	472.2 (0.7)	407.5 (1.0)	−15.9 (1.0)
Y	(1)	192.9 (0.7)	−131.1 (1.0)	−22.3 (1.1)
	(2)	178.6 (0.5)	−114.6 (0.7)	−27.0 (0.7)
	(3)	193.0 (1.0)	−128.4 (1.4)	32.7 (1.5)
	(4)	177.8 (0.6)	−112.7 (0.8)	36.1 (0.8)
Z	(1,3)	590.7 (0.6)	−261.8 (0.8)	145.3 (0.8)
	(2,4)	590.3 (0.5)	−294.2 (0.8)	−54.3 (0.8)

[a] Includes a phase angle of −2°.[37] [b] The standard deviations are given in parentheses.

Table 3. Orientation of the ^{31}P NMR Chemical Shift Tensor of *nido*-$Ru_4(CO)_{13}(\mu_3$-PPh), **2**, in the Crystal Axis System, given as Direction Cosines, with Standard Deviations in Units of the Least Significant Digit in Parenthesis[a]

	ppm	a	b	c
δ_{11}	888.8(13)	0.1695(10)	0.0236(36)	0.9852(1)
δ_{22}	293.7(11)	-0.9758(7)	0.1442(52)	0.1644(16)
δ_{33}	60.0(12)	0.1382(52)	0.9892(8)	−0.0475(35)

[a] The results are given for site 1, corresponding to *International Tables for X-ray Crystallography*; Kynoch Press: Birmingham, England, 1974; Vol. 1. The orientations for sites 2, 3, and 4 correspond to (−x, −y, z), (−x, y, −z), and (x, −y, −z), respectively.

where *i*, *j*, and *k* are in cyclic order and permutations of *X*, *Y*, and *Z*.

Once the CS tensors were constructed in the cube axis system, they were diagonalized to obtain the three principal components of the tensors in their principal axis system (PAS) and the direction cosines relating the PAS to the cube axis system. For the purpose of transforming the direction cosines into the crystal axis system, the symmetry properties of the space group were used to refine the relative orientations of crystal axis and cube axis systems.[38] The Euler angles relating the crystal axis system to the cube axis system are $\alpha = 94.6°$, $\beta = 90.5°$, and $\gamma = 91.3°$. Table 3 summarizes the results obtained from this analysis, giving the principal components and the orientation of the PAS in the crystal axis frame.

Assignment of the Phosphorus CS Tensors in the Molecular Axis System. Since there are four magnetically distinct sites in the unit cell, there are four possible ways to assign the chemical shift tensors to distinct sites, resulting in four different orientations in the molecular frame of reference. This is an inherent problem of single-crystal NMR spectroscopy for systems containing more than one magnetically distinct site,[37,39] and in the case of space group $P2_12_12_1$, this problem is well documented.[40] In such systems, assignments are often based on local symmetry arguments. However, during the course of the single-crystal NMR experiment we observed a clear orientation dependence of the cross-polarization efficiency. For several orientations, no cross-polarization was possible at all. Figure 6 shows the comparison of CP and single-pulse excitation under high-power proton decoupling (HP-DEC) for two orientations of the single crystal. At any given orientation of the single crystal in the applied magnetic field, the rate of cross-polarization is, *inter alia*, proportional to the ^{31}P,^{1}H dipolar second moment and hence proportional to the square of the ^{31}P,^{1}H dipolar coupling at that orientation.[20,41] The hydrogens closest to the phosphorus are the two ortho hydrogens (2.87 and 2.98 Å, resulting in a dipolar coupling constant, *R*, of 2060 and 1840 Hz), while the meta hydrogens (4.92 and 4.98 Å, *R* = 410 and 390 Hz) and para hydrogens (5.69 Å, *R* = 260 Hz) are much farther away. The closest intermolecular ^{31}P,^{1}H distance is 17 Å (*R* = 10 Hz), hence it is reasonable to consider the ^{31}P nucleus and the five protons of the directly bonded phenyl group as an isolated spin system.

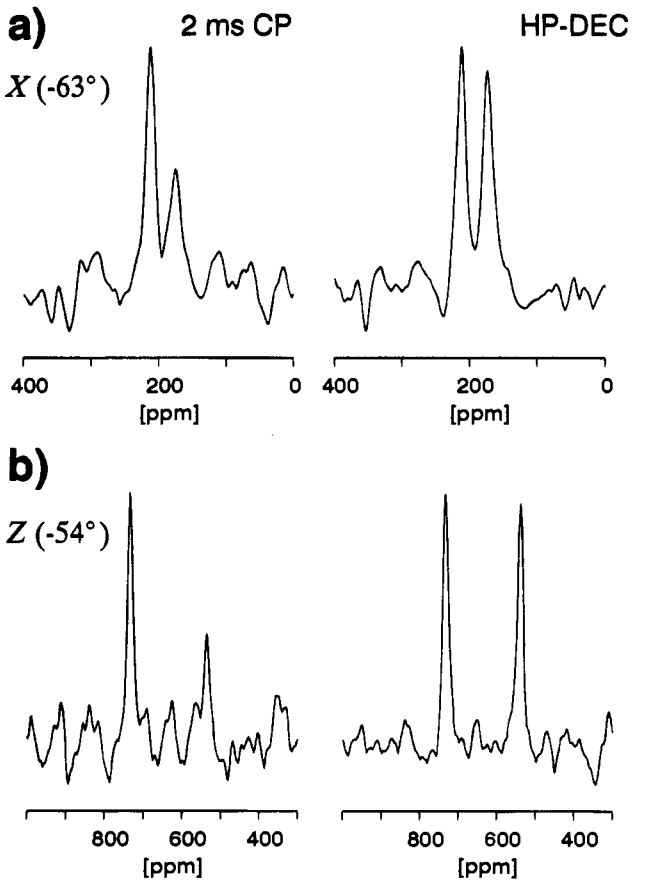

Figure 6. Dependence of the ^{31}P,^{1}H cross-polarization efficiency on orientation of the single crystal of *nido*-$Ru_4(CO)_{13}(\mu_3$-PPh) in B_0, corresponding to orientations *X*(−63°) (a) and *Z*(−54°) (b). The ^{31}P NMR spectra on the left were obtained after CP, using a 2 ms contact time, while those on the right were obtained with high-power ^{1}H decoupling.

A calculation of the phosphorus-proton dipolar second moment as a function of the crystal orientation shows that there indeed exist large differences between the different sites for rotations about the *X* and *Z* axes (Figure 7). In the following discussion we shall demonstrate how this information can be used to assign the four CS tensors to specific crystallographic sites. According to these calculations, at *X*(−63°), two crystallographic sites, 1 and 4, should result in strong peaks, while sites 2 and 3 are weak (*cf.* Figure 7). Suppose the four different chemical shift tensors obtained from the analysis are labeled

(38) Herzfeld, J.; Griffin, R. G.; Haberkorn, R. A. *Biochemistry* **1978**, *17*, 2711−8.

(39) Haeberlen, U. In *Advances in Magnetic Resonance*; Suppl. 1; Waugh, J. S., Ed.; Academic Press: New York, 1976.

(40) (a) Kempf, J.; Spiess, H. W.; Haeberlen, U.; Zimmermann, H. *Chem. Phys. Lett.* **1972**, *17*, 39−42. (b) Naito, A.; Ganapathy, S.; Akasaka, K.; McDowell, C. A. *J. Chem. Phys.* **1981**, *74*, 3190−7. (c) Janes, N.; Ganapathy, S.; Oldfield, E. *J. Magn. Reson.* **1983**, *54*, 111−21. (d) Naito, A.; Ganapathy, S.; Raghunathan, P.; McDowell, C. A. *J. Chem. Phys.* **1983**, *79*, 4173−82. (e) Naito, A.; McDowell, C. A. *J. Chem. Phys.* **1984**, *81*, 4795−803. (f) McDowell, C. A.; Naito, A.; Sastry, D. L.; Takegoshi, K. *J. Magn. Reson.* **1986**, *69*, 283−92. (g) VanWilligen, H.; Griffin, R. G.; Haberkorn, R. A. *J. Chem. Phys.* **1977**, *67*, 5855−60. (h) Marchetti, P. S.; Honkonen, R. S.; Ellis, P. D. *J. Magn. Reson.* **1987**, *71*, 294−302. (i) Ganapathy, S.; Chacko, V. P.; Bryant, R. G. *J. Chem. Phys.* **1984**, *81*, 661−8. (j) Kohler, S. J.; Klein, M. P. *J. Am. Chem. Soc.* **1977**, *99*, 8290−3.

(41) VanderHart, D. L. *J. Chem. Phys.* **1976**, *64*, 830−4.

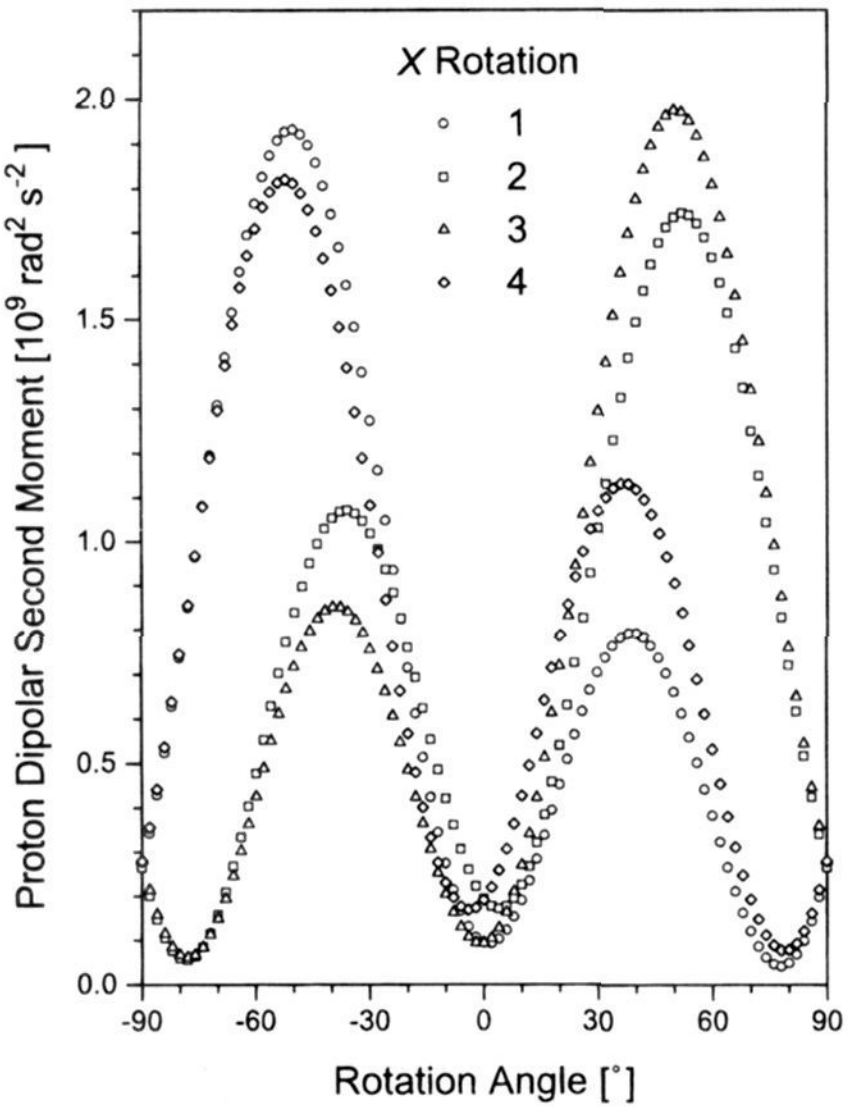

Figure 7. Dependence of the $^{31}P,^{1}H$ dipolar second moment in a crystal of *nido*-$Ru_4(CO)_{13}(\mu_3$-PPh) on the orientation of the crystal with respect to the external magnetic field, as calculated from the structure data.

A, *B*, *C*, and *D* in an arbitrary manner. At $X(-63°)$, the tensors *A* and *B* contribute to the strong signal, while *C* and *D* constitute the weak low-frequency peak (Figure 6). Hence, the calculations outlined above indicate that tensor *A* belongs either to site 1 or 4. Similarly, for $Z(-54°)$, the calculations indicate that sites 2 and 4 should be strong, and sites 1 and 3 should be weak. At this orientation, the CS tensors *B* and *C* yield the strong high-frequency peak, while *A* and *D* give rise to the weak low-frequency peak. Hence, tensor *A* belongs either to site 1 or 3. Combining the results for both orientations, $X(-63°)$ and $Z(-54°)$, only one assignment is in agreement with these observations: $A \leftrightarrow 1$, $B \leftrightarrow 4$, $C \leftrightarrow 2$, and $D \leftrightarrow 3$. It should be pointed out that, from all possible assignments, this assignment also best matches the local C_s symmetry about phosphorus.

The final result for the assignment of specific tensors to distinct sites is shown in Figure 8. To summarize: δ_{11} is ca. 8° off the direction of the P−C bond, while δ_{33} is perpendicular to the open face of the *nido*-cluster. The direction of intermediate shielding is within the plane of the open face, perpendicular to the P−C bond.

Theoretical Background. As indicated in Table 1, the phosphinidene group in ruthenium carbonyl clusters exhibits large ^{31}P chemical shift anisotropies, on average 600−1000 ppm. This large anisotropy primarily arises from the significant deshielding that results when B_0 is approximately parallel to the P−C bond. In the following discussion, we shall provide a qualitative explanation for this observation. Inevitably, we face with this kind of system the problem that it is presently beyond any quantitative theoretical treatment, *e.g.*, by *ab initio* MO calculations. Trends in the chemical shifts of nuclei other than protons are generally accounted for by considering variations in the paramagnetic contribution to nuclear magnetic shielding. Following Ramsey, the paramagnetic term for

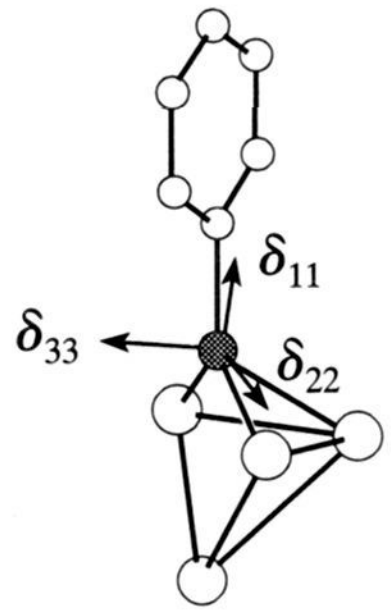

Figure 8. *Orientation of the phosphorus chemical shift tensor within* the molecular frame of *nido*-$Ru_4(CO)_{13}(\mu_3$-PPh), **2**, as determined from the single-crystal ^{31}P NMR experiment. The carbonyl groups are omitted for clarity.

nucleus A is[9]

$$\sigma^{p}_{\alpha\beta} = -\frac{\mu_0}{4\pi}\frac{e^2}{2m^2}\sum_{k\neq 0}(E_k - E_0)^{-1}\left[\langle\Psi_0|\sum_i l_{i\alpha}|\Psi_k\rangle \langle\Psi_k\left|\sum_i \frac{l_{iA\beta}}{r^3_{iA}}\right|\Psi_0\rangle + \langle\Psi_0\left|\sum_i \frac{l_{iA\alpha}}{r^3_{iA}}\right|\Psi_k\rangle \langle\Psi_k\left|\sum_i l_{i\beta}\right|\Psi_0\rangle\right] \quad (3)$$

where μ_0 is the permeability of free space, *e* and *m* are electronic charge and mass, respectively, α and β refer to the Cartesian components (*x*,*y*,*z*), r_{iA} is the position vector for electron *i*, and l_{iA} the electron angular momentum operator with respect to the observed nucleus A, whereas l_i is with respect to the chosen origin (*i.e.*, the gauge origin). Summations are taken over all electrons *i* and states *k*, except the ground state ($k = 0$), but including the continuum. E_k denotes the energy of the *k*th excited state. Because this theoretical approach involves perturbation theory, the system in the presence of an external magnetic field is described by mixing excited states into the description of the ground state. Therefore, the magnitude of σ^p depends on the difference in energies of the states involved. Generally, there is insufficient information available to evaluate eq 3, and a number of approximations are introduced.[42] Since the perturbation treatment mixes orbitals that are normally occupied with those that are unoccupied, the most common approximation is that the ground- and excited-state molecular wave functions, Ψ_k, can be approximated by high-lying bonding and low-lying antibonding orbitals, respectively. The mixing and hence the magnitude of σ^p will be larger, as the energy separation between corresponding occupied and unoccupied orbitals decreases, resulting in greater deshielding. However, the energy difference is not the only factor of importance in eq 3. The electron angular momentum operators, l_i, which act as rotation operators, ensure that only magnetic dipole allowed transitions contribute to σ^p. Qualitatively, the magnitude of σ^p along a particular direction will depend on how efficiently l_i mixes orbitals in a plane perpendicular to the rotation axis.[43] Obviously, symmetry considerations are important, as will be illustrated below. Also, the MOs connected by l_i only make a

(42) (a) Saika, A.; Slichter, C. P. *J. Chem. Phys.* **1954**, *22*, 26−8. (b) Pople, J. A. *J. Chem. Phys.* **1962**, *37*, 53−9 and 60−6. (c) Karplus, M.; Das, T. P. *J. Chem. Phys.* **1961**, *34*, 1683−92.

(43) (a) Jameson, C. J.; Gutowsky, H. S. *J. Chem. Phys.* **1964**, *40*, 1714−24. (b) Schatz, G. C.; Ratner, M. A. *Quantum Mechanics in Chemistry*; Prentice Hall: Englewood Cliffs, NJ, 1993; pp 92−5.

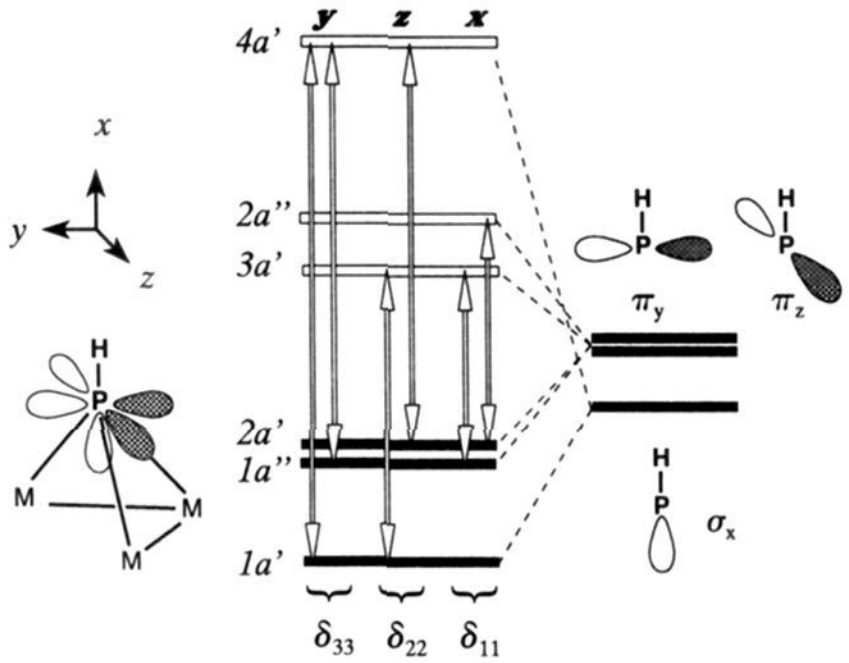

Figure 9. Simplified molecular orbital diagram of the frontier orbitals of a phosphinidene unit, HP^{2-}, and its interactions with an open triangle of transition metal fragments. Indicated by arrows are the magnetic dipole allowed transitions between occupied (solid levels) and empty orbitals (hollow levels), along with their respective polarizations.

large contribution to σ^p at A, if the AOs centered on A have large coefficients in these MOs. Finally, the inverse cube of the distance of the electron from the observed nucleus, r_{iA}, is responsible for the general observation that shielding is a local phenomenon. In the discussion which follows, we shall demonstrate that all of these factors should be considered even in a qualitative discussion.

Application of Ramsey's Theory to Cluster Compounds. The chemical, structural, and spectroscopic properties of transition metal clusters have often been described by applications of the extended Hückel molecular orbital method.[44] As outlined above, we are primarily interested in MOs with major contributions from phosphorus. Therefore, we shall restrict our interpretation to the frontier MOs (FMOs) of the phosphinidene unit, HP^{2-}, and consider their interactions with other molecular fragments. Similar, implicitly localized approaches have been successfully applied to the interpretation of the carbon CS tensor of methylene units bridging diiron compounds[45] and the nitrogen chemical shifts of imido ligands in mononuclear transition metal complexes.[46] The FMOs of HP^{2-} may conveniently be described as consisting of an sp-type lone pair directed opposite to the P−H bond and two p-type lone pairs perpendicular to the P−H bond. Such FMOs are isolobal to HC^{3-} and HB^{4-}, and according to their symmetry are commonly referred to as σ- and π-type orbitals (Figure 9).[44] There are also the σ- and σ^*-type orbitals associated with the P−H bond which we can neglect in our qualitative discussion.

From the simple MO scheme for an isolated HP^{2-} unit (Figure 9), the phosphorus nucleus in this species is expected to be very shielded: as in any linear molecule,[2b] the paramagnetic contribution to the direction parallel to the C_∞ axis is zero, while in the direction perpendicular to C_∞ only magnetic-dipole allowed transitions from the π-type lone pairs to the σ^* MO contribute to σ^p. Indeed, GIAO calculations show that the chemical shift for B_0 parallel and perpendicular to the P−H bond is −647 and −377 ppm, respectively. We may also compare HP^{2-} with the phosphaalkyne HC≡P, another species of the same molecular symmetry. From *ab initio* MO calculations using the IGLO method,[2c] the phosphorus chemical shift along the C_∞ axis of HCP is −692 ppm, slightly more shielded than the free atom. For B_0 perpendicular to the C_∞ axis significant deshielding occurs, $\delta_\perp = 302$ ppm ($\Omega = 994$ ppm). This arises from the availability of occupied and empty π and π^* orbitals, such that $\sigma \rightarrow \pi^*$ and $\pi \rightarrow \sigma^*$ transitions become possible. Also, the σ-type lone pair, which has no associated magnetic dipole allowed transition in HP^{2-}, gains the possibility of $n \rightarrow \pi^*$ transitions of relatively low energy, such that the lone pair contributes about one third of the deshielding found for HCP.[2c] Removal of the C_∞ axis by substitution, *cf.* H−C≡P and Ph−C≡P,[2c,47] also adds paramagnetic contributions along the molecular axis (about 300 ppm), illustrating the importance of symmetry. In the absence of a high-order rotation axis, the two π-type orbitals at phosphorus are also no longer degenerate, thus δ_{11} and δ_{22} may differ by several 100 ppm, as demonstrated experimentally for 2-(2,4,6-tri-*tert*-butylphenyl)-1-phosphaethyne, R−C≡P, $\delta_{11} = 229$, $\delta_{22} = 140$, $\delta_{33} = -274$ ppm,[48] and 2-(2,4,6-tri-*tert*-butylphenyl)-1-phospha-2-azaethynium tetrachloroaluminate, [R−N≡P]$AlCl_4$, $\delta_{11} = 308$, $\delta_{22} = 196$, $\delta_{33} = -273$ ppm.[49] In each of the molecules discussed so far, the direction of highest shielding is along the molecular axis.

The phosphinidene group found in transition metal clusters generally bridges three or four metal atoms. In order to discuss the results of our single-crystal NMR experiment on the *nido*-cluster **2**, we shall consider the effect of allowing a HP^{2-} fragment to interact with a triangular metal fragment, open at one side and hence possessing C_s symmetry as shown in Figure 9. Our qualitative discussion equally applies to complexes of C_{3v}, C_{4v}, or D_{4h} symmetry. The σ_x-type orbital of the HP^{2-} ligand can effectively overlap with the cluster frame. The phosphorus π_z-type orbital may simultaneously overlap with orbitals from two metal atoms, while the π_y-type orbital overlaps with orbitals on one of the metal atoms. Accordingly, due to the different strengths of interaction, the splitting of the two π-type orbitals into bonding and antibonding orbitals in the cluster differ. For the C_s cluster considered here, the bonding and antibonding orbitals resulting from the phosphorus σ_x, π_y, and π_z type orbitals belong to the irreducible representations a', a'', and a', respectively. Magnetic dipole allowed transitions between two a'-type orbitals are polarized perpendicular to the mirror plane, in the z direction, while transitions $a' \leftrightarrow a''$ or $a'' \leftrightarrow a''$ are polarized within the mirror plane, xy, without any further directional limitations. However, given the directions of the localized orbitals around phosphorus, not any arbitrary rotation will result in efficient transitions. For example, the transition between the highest occupied MO at P, $2a'$ with p_y character, and the second lowest unoccupied MO at P, $2a''$ with p_z character, is most efficient in the x direction. In Figure 9, arrows indicate the magnetic dipole allowed transitions between occupied and empty orbitals, along with their approximate polarization. The relative energies were obtained from EHMO calculations on *nido*-$Ru_4(CO)_{13}(\mu_3\text{-PH})$. This qualitative scheme reproduces the orientation of the phosphorus shielding tensor found for **2**: the orientation corresponding to least shielding, associated with the transitions of lowest energy, is predicted to

(44) (a) Hoffmann, R. *Angew. Chem., Int. Ed. Engl.* **1982**, *21*, 711−24. (b) Song, J.; Hall, M. B. *Inorg. Chim. Acta* **1993**, *213*, 75−82. (c) Halet, J.-F.; Hoffmann, R.; Saillard, J.-Y. *Inorg. Chem.* **1985**, *24*, 1695−1700. (d) Chesky, P. T.; Hall, M. B. *Inorg. Chem.* **1981**, *20*, 4419−25. (e) Bursten, B. E.; Cayton, R. H. *J. Am. Chem. Soc.* **1986**, *108*, 8241−9. (f) Bursten, B. E.; Cayton, R. H. *Polyhedron* **1988**, *7*, 943−54.

(45) Kim, A. J.; Altbach, M. I.; Butler, L. G. *J. Am. Chem. Soc.* **1991**, *113*, 4831−8.

(46) Bradley, D. C.; Hodge, S. R.; Runnacles, J. D.; Hughes, M.; Mason, J.; Richards, R. L. *J. Chem. Soc., Dalton Trans.* **1992**, 1663−8.

(47) Fleischer, U.; Kutzelnigg, W. *Phosphorus, Sulfur, Silicon* **1993**, *77*, 105−8.

(48) Duchamp, J. C.; Pakulski, M.; Cowley, A. H.; Zilm, K. W. *J. Am. Chem. Soc.* **1990**, *112*, 6803−9.

(49) Curtis, R. D.; Shriver, M. J.; Wasylishen, R. E. *J. Am. Chem. Soc.* **1991**, *113*, 1493−8.

be along the PH bond, while the direction of highest shielding is found to be perpendicular to the open face of the cluster.

Correlations between NMR Chemical Shifts and UV Transitions. The presence of the $(E_k - E_0)^{-1}$ term in Ramsey's equation indicates the possibility of correlations between NMR chemical shifts and the energy of electronic transitions, *e.g.*, determined from UV spectra. For example, it has been noted previously that the longer the wavelength of the UV−vis absorption of compounds in the series $[M_3(CO)_9(\mu_2\text{-H})_2(\mu_3\text{-PPh})]$, the more deshielded is the phosphorus nucleus: M = Os, pale yellow, δ_{iso} = 119 ppm; M = Ru, orange, δ_{iso} = 279 ppm; M = Fe, brown, δ_{iso} = 380 ppm.[50] Similarly, for a series of dinuclear phosphinidene complexes featuring trigonal planar phosphorus, $RP[ML_n]_2$, it has been found that the extreme deshielding observed for these species, with chemical shift values of 884−1362 ppm, exhibits an excellent linear correlation with the absorption of lowest energy in the UV−vis spectrum.[51] This finding has been rationalized using a simplified MO scheme involving a three-center four-electron π-system. Within this simplified MO picture, the deshielding has been correlated with the energy of the $\pi \rightarrow \pi^*$ transition between the highest occupied and lowest unoccupied MOs, HOMO and LUMO, respectively.[51] However, as previously pointed out by Grutzner,[52] care must be taken in making correlations between σ^p and energy gaps determined from electronic spectra since a purely rotational magnetic transition and a purely linear electronic transition are often mutually exclusive. Also, a HOMO−LUMO transition may not necessarily be responsible for deshielding, even if it is magnetic dipole allowed, as we shall demonstrate.

In many cases the HOMO and LUMO of phosphinidene complexes and other similar clusters are primarily centered at the metal atoms, with little contribution from the AOs of P (*i.e.*, they are metal−metal bonding and antibonding in nature). Whether phosphorus contributes to the HOMO or LUMO depends very much on the detailed nature of the cluster.[44,53] The EHMO calculations on *nido*-$Ru_4(CO)_{13}(\mu_3\text{-PH})$ indeed reveal a multitude of primarily metal centered occupied and empty orbitals with energies in between the simple P-based MOs shown in Figure 9. For the reasons indicated above, orbitals mainly localized on the metal atoms do not appear to contribute significantly to the phosphorus chemical shift. In fact, both HOMO and LUMO of the cluster belong to the a' irreducible representation, hence any magnetic dipole allowed HOMO−LUMO transition is polarized along z, which is not the direction of least shielding for phosphorus in **2**. Again, this provides further support for the qualitative description used here.

Even if phosphorus contributes to the HOMO or LUMO and the HOMO−LUMO transition is magnetically allowed, it may not contribute to σ^p. In the case of the dinuclear phosphinidene complexes with trigonal phosphorus, M−P(R)−M, the HOMO (a_2) of the three-center four-electron π-system possesses a nodal plane at phosphorus. Although the HOMO−LUMO transition ($a_2 \rightarrow b_2$) is magnetic dipole allowed with a polarization perpendicular to the MPM plane, we do not expect that this transition makes a large contribution to the paramagnetic term since the nodal plane at P should lead to small values of $\langle\Psi_0|l_{i\alpha}|\Psi_k\rangle$. The transition from the second-highest occupied MO (SOMO, b_2), the π orbital of lower energy, to the LUMO is not magnetic dipole allowed. Thus, within this three-center four-electron π-system neither of these transitions appears to be responsible for the deshielding. The magnetic dipole transitions $\sigma(MPM)(a_1,b_1) \rightarrow$ LUMO, $\sigma(PR)(a_1) \rightarrow$ LUMO, and SOMO $\rightarrow \sigma^*(MPM)(a_1)$ are allowed and would produce deshielding within the MPM plane, *i.e.*, under C_{2v} symmetry, along and perpendicular to the P−R bond. It is important to realize that in this case knowledge of the orientation of the phosphorus CS tensor would indicate whether the HOMO−LUMO $\pi \rightarrow \pi^*$ transition is of importance. If the $\pi \rightarrow \pi^*$ transitions were responsible for the deshielding observed experimentally, one deshielded component should be observed in the direction perpendicular to the molecular plane. However, if the other transitions are responsible, two deshielded but nondegenerate components should be observed within the molecular plane. Since the LUMO π^* is similar in character to an empty p orbital at phosphorus, it is interesting in this context that carbocations, featuring trigonal planar carbon, exhibit isotropic chemical shifts of ca. 300 ppm with respect to TMS.[54] The carbon chemical shifts of these species are at the high-frequency end of the carbon NMR chemical shift scale and have been attributed to $\sigma \rightarrow p_z$ transitions of very low energy.[2c,55] The two very deshielded directions lie within the molecular plane,[56] consistent with this argument. This description is in contrast to the common textbook interpretation which is invariably based on erroneous "charge" considerations.

Another interesting phenomenon observed in phosphorus NMR studies is the increase in shielding for unsaturated clusters of type **5**. This effect has previously been rationalized[35] in terms of a "ring-current" analogous to that in benzene, also causing a magnetic anisotropy. However, a crude estimation shows that, in order to produce such ring currents, several hundred delocalized electrons would be required.[57] Also, the CS tensor of **5** indicates a general shift of all principal components to lower frequencies, which is not what one would expect based on the magnetic anisotropy of ring currents. Qualitatively, in the context of the model proposed here, one would predict a stronger interaction between the unsaturated metal cluster fragment and the phosphinidene, causing wider gaps between the occupied and empty orbitals at phosphorus and hence a general attenuation of the paramagnetic contribution.

Using several examples we have demonstrated how crucial the experimental characterization of chemical shift tensors is in developing an understanding of phosphorus chemical shifts.

Acknowledgment. We wish to thank the Natural Sciences and Engineering Research Council of Canada (NSERC) for financial assistance in the form of equipment and operating grants (R.E.W. and A.J.C.). We thank Mr. Michael D. Lumsden for assistance with the GIAO shielding calculations and Professor Peter Pulay for providing us with the software necessary to perform the shielding calculations. Mr. Brian Millier is acknowledged for his ongoing support in the maintenance of the NMR spectrometers. All solid-state spectra were recorded at the Atlantic Region Magnetic Resonance Centre, which is also supported by NSERC.

JA9503286

(50) Huttner, G.; Knoll, K. *Angew. Chem., Int. Ed. Engl.* **1987**, *26*, 743−60.

(51) (a) Huttner, G. *J. Organomet. Chem.* **1986**, *308*, C11−3. (b) Huttner, G.; Lang, H. In *Multiple Bonds and Low Coordination in Phosphorus Chemistry*; Regitz, M., Scherer, O., Eds.; Georg Thieme Verlag, Stuttgart, 1990. pp 48−57.

(52) Grutzner, J. B. In *Recent Advances in Organic NMR Spectroscopy*; Lambert, J. B., Rittner, R., Eds.; Norell Press: Landisville, NJ, 1987; pp 17−42.

(53) Jaeger, J. T.; Field, J. S.; Collison, D.; Speck, G. P.; Peake, B. M.; Hähnle, J.; Vahrenkamp, H. *Organometallics* **1988**, *7*, 1753−60.

(54) (a) Olah, G. A.; Westerman, P. W. *J. Am. Chem. Soc.* **1973**, *95*, 7530−1. (b) Fyfe, C. A. *Solid State NMR for Chemists*; C. F. C. Press, Guelph/ON 1983; p 407.

(55) Schindler, M. *J. Am. Chem. Soc.* **1987**, *109*, 1020−33.

(56) Yannoni, C. S. *Acc. Chem. Res.* **1982**, *15*, 201−8.

(57) Johnson, C. E.; Bovey, F. A. *J. Chem. Phys.* **1958**, *29*, 1012−4.